Published online 4 November 2019

Nucleic Acids Research, 2020, Vol. 48, No. 1 ***e2***
doi: 10.1093/nar/gkz927

Gene knockdown in malaria parasites via non-canonical RNAi

Franziska Hentzschel[1,2,3], Vera Mitesser[1,2,3,†], Sabine Anne-Kristin Fraschka[4,†], Daria Krzikalla[1,2,3], Elena Herrera Carrillo[5], Ben Berkhout[5], Richárd Bártfai[4], Ann-Kristin Mueller[1,6,‡] and Dirk Grimm[2,3,6,7,*,‡]

[1]Heidelberg University Hospital, Center for Infectious Diseases / Parasitology, Im Neuenheimer Feld 324, 69120 Heidelberg, Germany, [2]Heidelberg University Hospital, Center for Infectious Diseases / Virology, Im Neuenheimer Feld 267, 69120 Heidelberg, Germany, [3]BioQuant Center, Heidelberg University, Im Neuenheimer Feld 267, 69120 Heidelberg, Germany, [4]Radboud University, Dept. of Molecular Biology, Geert Grooteplein 28, 6525 GA Nijmegen, The Netherlands, [5]Amsterdam UMC, University of Amsterdam, Department of Medical Microbiology, Meibergdreef 15, K3-110, 1105 AZ Amsterdam, The Netherlands, [6]German Center for Infection Research (DZIF), partner site Heidelberg and [7]German Center for Cardiovascular Research (DZHK), partner site Heidelberg

Received May 05, 2019; Revised October 01, 2019; Editorial Decision October 04, 2019; Accepted October 07, 2019

ABSTRACT

The lack of endogenous RNAi machinery in the malaria parasite *Plasmodium* hampers gene annotation and hence antimalarial drug and vaccine development. Here, we engineered rodent *Plasmodium berghei* to express a minimal, non-canonical RNAi machinery that solely requires Argonaute 2 (Ago2) and a modified short hairpin RNA, so-called AgoshRNA. Using this strategy, we achieved robust and specific gene knockdown throughout the entire parasite life cycle. We also successfully silenced the endogenous gene perforin-like protein 2, phenocopying a full gene knockout. Transcriptionally restricting Ago2 expression to the liver stage further enabled us to perform a stage-specific gene knockout. The RNAi-competent *Plasmodium* lines reported here will be a valuable resource for loss-of-function phenotyping of the many uncharacterized genes of *Plasmodium* in low or high throughput, without the need to engineer the target gene locus. Thereby, our new strategy and transgenic *Plasmodium* lines will ultimately benefit the discovery of urgently needed antimalarial drug and vaccine candidates. Generally, the ability to render RNAi-negative organisms RNAi-competent by mere introduction of two components, Ago2 and AgoshRNA, is a unique paradigm that should find broad applicability in other species.

INTRODUCTION

Protozoan *Plasmodium* parasites and the disease they cause in humans, malaria, remain a global health burden that claims hundreds of thousands of lives each year. The implementation of effective prevention or intervention modalities is thus highly desirable but remains challenging without a better dissection and understanding of the function of *Plasmodium*-specific genes. Consequently, numerous efforts have previously been undertaken to establish methodologies for gene manipulation and annotation in *Plasmodium* (1). Genome-wide screens revealed that approximately 45 to 50% of genes are essential for the pathological asexual blood stage development, and are thus refractory to traditional targeted gene deletion (2,3). A variety of conditional systems were developed to study these essential genes, e.g. the GlmS ribozyme system or the knock-sideways system (reviewed in (1)). These methodologies enable the inducible depletion of targets and in many cases also fine-tuning of gene expression in order to investigate dose-dependent effects. Together, these tools have thus greatly advanced our knowledge of *Plasmodium* and malaria biology in recent years. Yet, many of these strategies have variable, gene-dependent success rates and often are not adapted to the murine *Plasmodium* model, especially for studying gene function in the extra-erythrocytic stages (1). It is therefore desirable to develop additional genetic tools that complement the existing repertoire, in order to also characterize the ∼30% of all *Plasmodium* genes that remain annotated as having unknown function (www.plasmodb.org). Collectively, this motivated us to try and establish a new method that allows for

*To whom correspondence should be addressed. Tel: +49 6221 5451339; Fax: +49 6221 5451481; Email: dirk.grimm@bioquant.uni-heidelberg.de
†The authors wish it to be known that, in their opinion, the second and third authors should be regarded as Joint Second Authors.
‡Equal Senior Authors.
Present address: Franziska Hentzschel, Wellcome Centre for Integrative Parasitology, Glasgow Biomedical Research Centre - Room B621, University of Glasgow, 120 University Place, Glasgow G12 8TA, Scotland.

specific gene modulation in selected stages of *Plasmodium*, e.g. insect stages (oocysts, sporozoites), without a necessity for direct engineering of targeted loci.

In most eukaryotes, a respective tool is available in the form of RNA interference (RNAi), an endogenous pathway for gene regulation on the mRNA level that can be usurped by using small interfering or short hairpin RNAs (siRNAs or shRNAs, respectively) as exogenous RNAi triggers (4). However, *Plasmodium* species lack the canonical RNAi machinery, including the key enzymes Dicer that processes transcribed shRNAs into siRNAs, as well as Argonaute 2 (Ago2) that, when loaded with the siRNA, binds and cleaves target mRNA (5). Interestingly, though, a non-canonical RNAi pathway has recently been described in mammalian cells that requires only Ago2 to process a special type of shRNAs (6,7). These so-called AgoshRNAs have a shorter stem and loop than conventional shRNAs, which prevents their recognition by Dicer and instead facilitates direct loading into, and processing by, Ago2 (7,8). The resulting protein-RNA complex then binds to a complementary target mRNA and causes its cleavage and degradation.

Here, we introduced this minimal RNAi machinery into the rodent model parasite *P. berghei* and thus created RNAi-competent *Plasmodium* strains that permit inhibition or fine-tuning of gene expression on the mRNA level.

MATERIALS AND METHODS

Ethics statement

All animal experiments were performed according to European regulations concerning FELASA category B and GV-SOLAS standard guidelines. Animal experiments were approved by German authorities (Regierungspräsidium Karlsruhe, Germany), § 8 Abs. 1 Tierschutzgesetz (TierSchG) under the license G-260/12 and were performed according to National and European regulations. For all experiments, female C57BL/6 (6- to 8-week-old) and outbred mice (NMRI, 8- to 10-week-old) were purchased from Janvier laboratories, France. All mice were kept under specified pathogen-free (SPF) conditions within the animal facility at Heidelberg University (IBF).

Maintenance of parasite life cycle

Unless mentioned differently, routine passage of blood stage *P. berghei* parasites and experiments were performed using NMRI mice infected by intraperitoneal injections. For mosquito infections, *Anopheles stephensi* mosquitoes were reared at 28°C and 80% humidity under a 14 h/10 h light/dark cycle and fed on 10% sucrose/PABA (para-aminobenzoic acid) solution. Adult mosquitoes were fed on parasite-infected (gametocytemic) mice and maintained at 21°C and 80% humidity. Midguts were dissected on day 12–14 and salivary glands to isolate sporozoites on day 18 after feeding. To determine blood-stage growth, C57BL/6J mice (Janvier) were infected intravenously with 10^3 infected red blood cells (iRBCs) or 10^4 sporozoites, and parasitemia was monitored from 3 to 15 days post-infection by examining Giemsa-stained blood smears. Animals were sacrificed when they exhibited signs of severe disease.

Cloning

All PCRs were performed with Phusion Hot Start II polymerase (Thermo Fisher Scientific, USA) in GC buffer supplemented with DMSO at standard conditions unless described differently. *Plasmodium* genes were amplified at a reduced extension temperature of 68°C. Gibson assembly was performed using the Gibson Cloning Mastermix (NEB, USA) according to instructions of the manufacturer, but at a reduced incubation temperature of 40°C. Oligonucleotides were annealed by incubation of equal amounts of complementary forward and reverse oligonucleotides in NEB2 buffer (NEB) at 95°C for 5 min followed by a slow cool down to room temperature. Primer sequences are listed in Supplementary Table S1.

To express the GFP from *Pb*GFPcon in cell culture, the *gfp* coding region was amplified from genomic DNA using primers P1/P2 and cloned into a self-complementary AAV vector plasmid via *Xho*I/*Nhe*I under the Cytomegalovirus (CMV) promoter (9). For all *Plasmodium* transfections, a modified version of the published vector pBAT-SIL6 (10) was used in which the mCherry open reading frame was removed by *Xba*I/*Blp*I digest and ligation to annealed oligonucleotides P3/P4. Similarly, the *gfp* open reading frame was replaced by a multiple cloning site through *Nde*I/*BamH*I digest and ligation to annealed oligonucleotides P5/P6, yielding pBAT-SIL6-MCS. The vector pBAT-SIL6-Ago2 used for integration of the Ago2 expression cassette into *SIL6* (PbANKA_10_v3:524240..525356 bp) was generated by amplifying a previously published, codon-optimized and N-terminally FLAG-tagged version of Ago2 (11) using primers P7/P8 and cloning it into pBAT-SIL6-MCS via standard restriction digest with *Nde*I/*BamH*I. To drive Ago2 expression by the *LISP2* promoter (5′*LISP*), the *HSP*70 promoter from pBAT-SIL6-Ago2 was excised by *Spe*I/*Swa*I digest and a previously published, about 1 kb long region upstream of the *LISP2* gene (12) (PbANKA_10_v3:190,309..191,296; amplified from genomic DNA with primers P9/P10) was inserted via Gibson assembly, resulting in pBAT-SIL6–5′*LISP2*-Ago2.

Plasmids pBAT-SIL6-mCherry-*Pb*U6 and pBAT-SIL6-*Pb*U6int were cloned for episomal expression or stable integration of AgoshRNAs, respectively. The *Pb*U6 promoter region (PbANKA_13_v3:2 056 836..2 057 417) was amplified from genomic DNA using primers P10/P11 and cloned into pBAT-SIL6-MCS by standard restriction digest with *Xho*I/*Xma*I. For creation of pBAT-SIL6-mCherry-*Pb*U6, the vector was then *Swa*I/*BamH*I-digested and the mCherry cDNA, amplified using primers P13/P14, was integrated via Gibson assembly. To generate pBAT-SIL6-*Pb*U6int, the left homology region of SIL6 as well as the 5′*HSP70* region from pBAT-SIL6-MCS-*Pb*U6 were removed by *NgoM*VI/*BamH*I digest and ligation to annealed oligonucleotides P15/P16. The remaining right homology region of SIL6 as well as the 3′ untranslated regions (UTRs) of Ago2 and the selection cassette (3′*PbDHFS-FPGS* and 3′*PbDHFR-TS*) served as homology arms for integrating the *Pb*U6 cassette along with the selection marker into *Pb*Ago2. Since this construct design was inefficient at integrating AgoshRNAs due to an internal homologous re-

gion, this internal region was removed from the vector by *Xho*I/*Bcl*I digest and replaced with a duplicate of the Ago2 3′UTR (*3′PbDHFS-FPGS*) region that was PCR-amplified using primers P17/P18. To further avoid unwanted recombination events, the left homology arm was additionally shortened by removing the 3′*PbDHFS-FPGS* region via *BamH*I/*Sac*I digest and ligation of the backbone to annealed oligonucleotides P19/P20, resulting in pBAT-SIL6-*PbU6*int V2.

Design and cloning of AgoshRNAs

AgoshRNA target sequences were identified using the 'siRNA wizard' tool (http://www.invivogen.com/sirnawizard/design.php), by searching for 19 nt long target sequences that start with an A and end with a T. The antiparallel sequence (antisense) of this target sequence then precedes a 5 bp-long loop sequence, followed by the sense sequence. In the initial set of αGFP-AgoshRNAs, the loop sequence consisted of the next 5 bp following the target sequence, essentially expanding it to 24 nt. More recent publications demonstrated, however, that such an extended target sequence does not improve efficiency (13). Thus, the loop sequence for all following AgoshRNAs consisted of CTTCA. To create an initial A–C and a terminal G–U mismatch, the first and the last nucleotide of the sense sequence were replaced by a G and a C, respectively. For cloning behind the *Pb*U6 promoter, four additional Ts were added to the AgoshRNA to serve as termination signal. The resulting AgoshRNAs were ordered as two complementary oligonucleotides with initial and terminal overhangs that match the respective overhangs of the *Bbs*I-digested target vector (Supplementary Figure S1). All AgoshRNA target sequences are listed in Supplementary Table S2, together with their GC content. The forward and reverse oligonucleotides were annealed by incubating 5 μM of each oligonucleotide in 50 μl H_2O supplemented with 1× NEB2 buffer for 5 min at 95°C, followed by a slow cool down to room temperature. For *in vitro* screens in cultured cells, AgoshRNAs were cloned as annealed oligonucleotides into the *Bbs*I-digested plasmid pbs-sds-CMV-mCherry-U6 kindly provided by Kathleen Börner (Heidelberg University Hospital, Center for Infectious Diseases, Virology). For expression in *Plasmodium*, AgoshRNAs were cloned into the *Bbs*I-digested pBAT-SIL6-mCherry-*Pb*U6 or pBAT-SIL6-*Pb*U6int vector.

Cell culture screen of AgoshRNAs

AAV vectors encoding GFP, AgoshRNA or shRNA were produced by triple-transfection of HEK293T cells as described previously (14), using the vector plasmids described above and AAV-DJ as capsid (15). Two days after transfection, cells were harvested and lysed by five freeze-thaw cycles followed by 1 min sonification and removal of cellular debris by centrifugation at full speed for 10 min. Wild-type or Dicer-deficient MEF cells were transduced with 5 μl supernatant. GFP fluorescence in mCherry-positive cells was measured via flow cytometry of trypsinized cells three days after transduction.

Transfection of parasites

P. berghei blood-stage parasites were transfected as described previously (16), using 10–20 μg of ethanol-precipitated DNA resuspended in 10 μl phosphate-buffered saline (PBS). Vectors for integration were linearized with *Pvu*I prior to transfection, while vectors used for episomal expression of AgoshRNAs were transfected as circular plasmids. One day post-transfection, the drinking water of the mice was supplemented with pyrimethamine (70 μg/ml). In the case of stable integration into the genome, single clones were obtained by limited dilution. Subsequently, the resistance marker was recycled by negative selection with 5′fluorocytosine (5′FC) as described previously (17). Briefly, the resistance marker also included the gene yFCU (yeast cytosine deaminase/uridyl phosphoribosyl transferase), which renders parasites sensitive to the drug 5′FC. Upon 5′FC drug pressure, only parasites will survive that have removed the selection marker by homologous recombination using two homologous regions that flank the cassette.

Diagnostic PCRs for genotyping

Parasites were obtained by bleeding mice with a parasitemia >1%. White blood cells were removed by CF11 (Thermo Fisher Scientific) column filtration (18). After lysis of erythrocytes in 0.2% saponin/PBS, the pelleted parasites were resuspended in 200 μl PBS. Genomic DNA was isolated using the DNA Blood & Tissue Kit (Qiagen, Germany) according to the supplied protocol. To verify integration of Ago2 expression cassettes, parasites were genotyped via PCR using primers P17/P18, P17/P19 or P18/P20 for wild-type, 5′ integration and 3′ integration, respectively. Successful negative selection was verified using primers P18/P21. After integration of the *Pb*U6-AgoshRNA cassette into *Pb*Ago2 or Pb_{LISP2}Ago2, lines were genotyped using primers P18/P20 (3′ integration) and P18/P21 (parental locus).

Western blotting

For western blotting of mixed blood stages, parasites were purified via CF11 column filtration (18). Schizont-enriched parasites were obtained as described previously (16). In both cases, the parasite pellet was resuspended in RIPA buffer and incubated for 1 h on ice, during which it was vortexed at regular intervals. Protein concentration was measured using the Qubit Protein Assay kit (Thermo Fisher Scientific) according to the provided instructions. Western blots were performed under standard conditions, using 5% milk to block membranes and incubation with primary antibodies (either for 2 h at room temperature or overnight at 4°C) and horseradish peroxidase-(HRP-)coupled secondary antibodies (1 to 2 h incubation at room temperature). Antibodies were diluted in 5% milk as follows: Mouse-anti-HSP70 (19), rat-anti-Ago2 (clone 11A9) (20) and mouse-anti-GFP (Cat. No. 14-6674-82, eBioscience Inc., USA): 1:500; mouse-anti-EXP1 (21): 1:1,000; HRP-linked anti-mouse (Jackson Immuno-Research, USA) and HRP-linked anti-rat (GE-Healthcare, UK): 1:10 000.

Liver-stage development

To assess liver-stage development, salivary gland sporozoites were added to HuH7 cells and incubated for 90 min at 37°C to allow time for invasion. Remaining sporozoites were washed off and cells were incubated for 48 h at 37°C and 5% CO_2. Liver stages were fixed by addition of ice-cold methanol, blocked with 10% fetal calf serum/PBS and incubated with primary antibody against parasitic HSP70 (19) (mouse) (dilution 1:100) or EXP1 (21) (rat) (dilution 1:33) and, if applicable, rabbit-anti-GFP (dilution 1:125) (Cat. No. PA146326, Thermo Fisher Scientific) or mouse-anti-FLAG (dilution 1:125) (Cat. No. F1804-1MG, Sigma-Aldrich, Germany) followed by Alexa488- or Alexa546-conjugated secondary antibodies (dilution 1:300) (Life Technologies, UK).

Microscopy

Microscopy of blood stages, oocysts, sporozoites as well as liver stages was performed on a Zeiss wide-field Fluorescence Axiovert 200M microscope. Within experiments, image acquisition settings, exposure times and processing steps were kept constant. GFP fluorescence intensities per parasite and size of liver stages were quantified using ImageJ.

PPLP2 knockdown, exflagellation events and exflagellation frequency

To increase gametocytemia, mice were pretreated with phenylhydrazine (PHZ; 2 μg per mouse in 200 μl PBS, intraperitoneally [i.p.] injected) (22). Two days later, mice were infected i.p. with AgoshRNA-transfected *Pb*Ago2. A drop of blood was collected from tail veins 4–5 days after *Plasmodium* infection, mixed with 2 μl of xanthurenic acid (50 μM), covered with a coverslip and incubated for 12 min at room temperature. Exflagellations were observed under a microscope (40× objective) and scored for 2.5 min according to the presence of free flagella (normal) or one or two thick superflagella (abnormal). This procedure was repeated until at least 100 exflagellations per *PbAgo2* + AgoshRNA line could be observed. To quantify exflagellation rates, PHZ-pretreated mice were infected intravenously with 2×10^6 iRBCs and at least three exflagellation assays per mouse were performed 4 days post-infection. Fields of view were counted additionally to determine exflagellation per field of view. Exflagellation rates were always normalized to the exflagellation rate of *Pb*Ago2 + scr-AgoshR determined in parallel.

Quantitative real-time-(qRT-)PCR of PPLP2

For PPLP2, blood of PHZ-pretreated and *Pb*Ago2 + AgoshRNA-infected mice was purified over CF11 columns and lysed with saponin, and the parasite pellet was resuspended in Qiazol (Qiagen). Total mRNA was isolated from these samples using the miRNeasy kit (Qiagen) according to the manufacturer's instructions. Quantitative real-time PCR was performed using the Power SYBR® Green PCR Master Mix (Applied Biosystems, USA) and the primer pairs P22/P23 (PPLP2) and P26/P27 (gametocyte marker PBANKA_0619200 [PB000198.00.0] (23), housekeeper). Efficiencies of each primer pair were determined using serial dilutions of a template and relative quantifications of each target were calculated as described previously (24).

RNA-Seq library preparation

To prepare samples for RNA-Seq, mice were bled at a parasitemia of ∼1–2%, leukocytes were removed from the blood by CF 11 column filtration and iRBCs were cultured to enrich for schizonts as described previously (16). To ensure highest possible synchrony of the cultures, the incubation was always started at 1:30 pm and samples were harvested 18 h later (7:30 am). Blood from the culture was pelleted for 8 min at 400 × g, and the blood was resuspended in 3 ml RLT buffer (Qiagen) supplemented with 1% β-mercaptoethanol.

Total RNA was extracted using the RNeasy Mini Kit (Qiagen, including on-column DNase treatment and RNA clean-up) and PolyA-selected using the Oligotex mRNA Mini Kit (Qiagen) according to the manufacturer's instructions. PolyA-selected RNA was tested for genomic DNA contamination via qPCR and additionally treated twice with Ambion TURBO DNase (Thermo Fischer Scientific) to eliminate remaining genomic DNA. Two micrograms of PolyA-selected total RNA equivalent were fragmented by alkaline hydrolysis (5x fragmentation buffer: 200 mM Tris-acetate pH 8.2, 500 mM potassium acetate, 150 mM magnesium acetate) for 2 min at 85°C in 250 μl volume as described (25), precipitated and further processed for strand-specific RNA-Seq as also described (26). In short, first-strand cDNA synthesis was performed using AT-corrected Random N9 primers (76% AT) and in the presence of 0.2 μg Actinomycin D (Thermo Fisher Scientific) to prevent unwanted DNA-dependent second-strand cDNA synthesis. During second-strand synthesis, dTTPs were replaced with dUTPs. For each sequencing library, 5 ng of double-stranded cDNA were end-repaired, extended with 3′ A overhangs, ligated to barcoded NextFlex adapters (Bio Scientific, USA) and treated with USER enzyme (NEB) to induce dUTP-dependent second strand-specific degradation. Subsequently, libraries were amplified using KAPA HiFi HotStart ready mix (KAPA Biosystems, USA), NEXTflex primer mix (Bio Scientific) and the following PCR program: 98°C for 2 min; 4 cycles of 98°C for 20 s, 62°C for 3 min; 62°C for 5 min. Amplified libraries were gel size-selected for 300–400 bp using 2% E-Gel Size Select agarose gels (Thermo Fischer Scientific) and a second time amplified by performing eight additional cycles as described above. Adapter dimer depletion and DNA clean-up were performed using Agencourt AMPure XP beads (Beckman Coulter, USA) and a 1:1 library:beads ratio.

High-throughput sequencing and data analysis

Strand-specific RNA-Seq libraries were sequenced on the Illumina NextSeq 500 system to obtain 75 bp single-end reads (TruSeq SR Cluster Kit v2, Illumina, USA). 75 bp reads were mapped against the annotated *P. berghei*

ANKA transcriptome from PlasmoDB version 26 (http://www.plasmodb.org) and the *gfp* coding sequence encoded by the *Pb*GFPcon parasite line (27) using BWA samse (version 0.7.12-r1039, http://bio-bwa.sourceforge.net/) (28). Single-end RNA reads were filtered to mapping quality ≥15 (samtools version 1.2) and only uniquely mapped reads (between 5.3 and 8.1 million reads) were used for further analysis.

To assess RNA abundance of each gene, only reads aligned to the sense strand (FLAG16) were considered. Tags were counted for all transcripts (excluding mitchochondrial RNA, apicoplast RNA and RNAs without PolyA tail such as rRNAs and tRNAs) and offset by +1 to avoid division by zero while calculating fold-change in expression. Transcript counts were normalized to the amount of reads per kb per million mapped reads (RPKM). Correlations between datasets were calculated and plotted with R studio (R version 3.2.2, standard packages, https://www.r-project.org/).

Statistical analysis

All statistical analysis was done using GraphPad Prism 5.0 (http://www.graphpad.com). Experiments were performed in biological duplicates or triplicates on separate occasions (for each experiment, the precise number of biological replicates n is indicated in the figure legend). Where appropriate, data was compared to a control using a two-tailed Student's *t*-test (if the experiment included only two groups) or a one-way ANOVA or non-parametric Kruskal–Wallis test (if the experiment included three or more groups). The statistical method used for each data analysis is indicated in the respective figure legend. One-way ANOVA or Kruskal–Wallis tests were followed by Dunnett's post test (if samples were compared to a single control) or by Bonferroni's multiple comparison test (if selected sets of samples were compared).

RESULTS AND DISCUSSION

AgoshRNAs can silence GFP in the absence of Dicer

As the concept of Dicer-independent shRNAs is still fairly new, we initially designed and prescreened a panel of AgoshRNAs in cell lines that lack Dicer expression. As proof-of-concept target, we chose a *gfp* transgene that is stably and ubiquitously expressed in a *P. berghei* reporter strain that we used in later experiments, *Pb*GFPcon (10,27). Consequently, we designed four different αGFP-AgoshRNAs (αGFP-AgoshR1–4) according to published guidelines (7,8,29) (Figure 1A, Supplementary Figure S1, Table S2) and assessed their *gfp* knockdown efficiency in wild-type versus Dicer-deficient mouse embryonic fibroblasts (MEF) via flow cytometry. As these cells are hard to transfect, we co-transduced them with two Adeno-associated viral (AAV) vectors (15), one encoding an AgoshRNA and the other the *gfp* transgene (subcloned from *Pb*GFPcon).

In wild-type MEF, αGFP-AgoshR2 as well as a conventional shRNA (αGFP-shR, positive control) significantly reduced GFP fluorescence compared to a scrambled (scr) AgoshRNA as negative control (Figure 1B, black bars). In contrast, αGFP-shR failed to inhibit GFP expression in Dicer-deficient cells, reflecting the dependency of traditional shRNAs on Dicer processing (Figure 1B, grey bars). Remarkably, in these Dicer-deficient cells, αGFP-AgoshR2 remained capable of reducing GFP fluorescence by ∼50%, confirming that AgoshRNAs can act independently of Dicer. Interestingly, we noted a slightly but significantly higher activity of all four AgoshRNAs in the absence of Dicer. Such an effect has been observed previously and may be attributed to decreased competition of the AgoshRNAs with endogenous small RNAs for Ago2 loading (13). We thus conclude that we have successfully designed and identified an AgoshRNA that potently suppresses *gfp* expression in the absence of a canonical RNAi machinery *in vitro*.

AgoshRNAs permit fine-tuning of *gfp* expression in an Ago2-expressing *P. berghei* line

Our next aim was to introduce a minimal RNAi machinery into *Plasmodium*. To this end, we stably integrated an Ago2 cDNA under the control of the strong, ubiquitous *HSP70* promoter (30) into the SIL6 locus in the genome of *Pb*GFPcon (Supplementary Figure S2A, see Materials and Methods for details), yielding the Ago2-expressing *P. berghei* line *Pb*Ago2. Diagnostic PCRs verified correct integration of the expression cassette in two independent clones (A and B, Supplementary Figure S2B). As expected for the *HSP70* promoter, both clones express Ago2 constitutively, as proven by Western blotting and immunofluorescence analysis in blood or liver stages, respectively (Figure 2A-B). Inoculation of mice with sporozoites or infected red blood cells revealed a slight negative impact of stable Ago2 expression on parasite blood-stage growth, accompanied by increased survival of infected mice (Supplementary Figure S2C-D). Additionally, mosquito infectivity was substantially reduced in *Pb*Ago2 (Supplementary Figure S2E and F). Notably, we found no evidence of defects in *in vitro* liver-stage development (Supplementary Figure S2G). Thus, a minor pre-patency delay of blood-stage infection after sporozoite inoculation can likely be attributed to the decreased asexual replication rate (Supplementary Figure S2D). As a whole, the fact that we detected liver, blood as well as mosquito stages implies that *Pb*Ago2 can complete all stages of the parasite's life cycle.

We subsequently tested whether AgoshRNA expression in *Pb*Ago2 would mediate targeted gene knockdown. Therefore, we transfected *Pb*Ago2 or *Pb*GFPcon wild-type with an episomal vector encoding αGFP-AgoshR2 or a scrambled control (scr-AgoshR) under the *P. berghei* U6 promoter (31). Furthermore, we included an mCherry reporter to permit microscopic identification of positive transfectants. Analysis of schizont-enriched samples (Figure 2C and D) revealed a marked GFP reduction in *Pb*Ago2 transfected with αGFP-AgoshR2, as compared to the scr-AgoshR control. Congruent with this, quantification of the GFP fluorescence of individual parasites showed a strong decrease in ring stages, trophozoites and gametocytes (sexual stages) (Figure 2D, Supplementary Figure S3, Figure S4A–C). GFP fluorescence in *Pb*GFPcon (lacking Ago2) was unaffected by αGFP-AgoshR2, further corroborating that canonical RNAi is not functional in *P. berghei*.

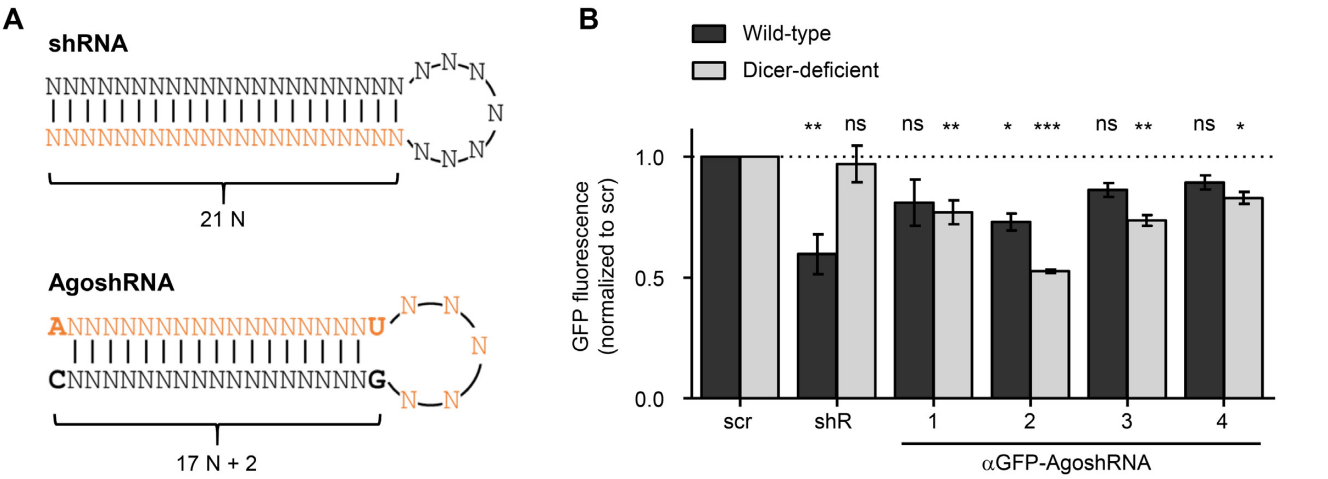

Figure 1. AgoshRNAs can silence GFP in absence of Dicer. (**A**) Structure of shRNAs (upper panel) and AgoshRNAs (lower panel). The sequence complementary to the target sequence (i.e. the shRNA/AgoshRNA guide sequence) is indicated in orange. For AgoshRNAs, this sequence can continue across the loop. Fixed nucleotides at the beginning and the end of the stem are indicated in bold. The length of the stem is indicated below the scheme. Sequences of the AgoshRNA antisense strands are listed in Supplementary Table S2. (**B**) GFP fluorescence of wild-type (black) or Dicer-deficient (gray) MEFs expressing GFP and αGFP-shRNA (shR) or αGFP-AgoshRNAs normalized to scr-AgoshR (scr). Stars indicate significance of difference to respective scr control. Shown are means ± SEM ($n = 3$). Statistics: (**B**) One-way-ANOVA. ns, non-significant; *$P < 0.05$; **$P < 0.01$; ***$P < 0.001$.

With an approximately 40-fold decrease in GFP fluorescence, αGFP-AgoshR2 was far more potent in *Pb*Ago2 than in Dicer-deficient MEF where its effect was only two-fold (Figure 1B, grey bars). We thus asked whether the other three αGFP-AgoshRNAs, which were only mildly active in the initial screen, would also trigger more robust GFP knockdown in *Pb*Ago2. Indeed, following transfection of *Pb*Ago2 A with αGFP-AgoshR1, 3 or 4, we observed an increased, five- to 13-fold GFP inhibition (Figure 2E, Supplementary Figure S3, Figure S4D–G). Consistent with its superior performance in MEF (Figure 1B), αGFP-AgoshR2 was also most potent in *Plasmodium*. Hence, the non-canonical RNAi machinery that we have introduced into *P. berghei* is not only robust, but also enables variable degrees of target mRNA knockdown that are determined by AgoshRNA efficiency. This additional feature is particularly useful to study dose-dependent effects of gene knockdowns yielding intermediate phenotypes. In addition, our approach does not require engineering of the target sequence, in contrast to other available gene modification systems. This feature renders RNAi-competent *Plasmodium* especially interesting for the study of genes that are refractory to tagging.

AgoshRNA-mediated gene silencing results in minimal off-targeting

A recurrent concern with RNAi approaches is inhibition of off-target mRNAs, which can be induced by the guide or the passenger strand of the RNAi trigger, and which can mask the phenotype of the on-target knockdown (32,33). As compared to traditional shRNAs, AgoshRNAs have a lower risk of off-targeting due to cleavage of their passenger strand during processing (7,34). Still, we assessed whether αGFP-AgoshRNA expression affected global transcript levels in *P. berghei*. We thus performed RNA-Seq on schizont-enriched blood-stage samples of the parental *Pb*GFPcon and *Pb*Ago2 expressing either scr-AgoshR or αGFP-AgoshR2. Intriguingly, we found remarkable differences between the transcriptome of the parental *Pb*GFPcon and *Pb*Ago2 (with or without AgoshRNA). Specifically, in *Pb*Ago2, we observed a significantly lower abundance of female gametocyte-specific transcripts that prior work had shown to be down-regulated upon deletion of DOZI (development-of-zygote-inhibited) (Supplementary Figure S5, Table S3) (35). In a complex together with CITH (homolog of worm CAR-I and fly Trailer Hitch), DOZI mediates translational repression of zygote-specific mRNAs in female gametocytes (35). Notably, male gametocyte-specific transcripts or other female-gametocyte-specific transcripts, including members of the DOZI/CITH complex, were not affected (Supplementary Figure S5), suggesting that Ago2 expression does not influence gametocyte formation/maturation. Since Ago2 is known to interact with DDX6 (also called Rck/p54), the human homolog of DOZI (36), it is tempting to speculate that an Ago2-DOZI interaction and ensuing changes in zygote-specific gene expression contribute to the reduced growth and mosquito infectivity of *Pb*Ago2 parasites described earlier (Supplementary Figure S2E).

We then further compared the transcriptome of *Pb*Ago2 expressing the αGFP-AgoshR2 to *Pb*Ago2 expressing the scr-AgoshR for any off-target effects that may have been caused by the expression of an active AgoshRNA. With GC contents of 42.1% (scrambled control) versus 47.4% (αGFP AgoshR2), we considered these two AgoshRNAs sufficiently similar to make this comparison fair and unbiased (see also Supplementary Table S2 for the GC contents of all AgoshRNAs used in this work). Importantly, we found that the two parasite lines displayed largely similar gene expression patterns. The most prominent change observed was the expected, about 10-fold reduction in *gfp* mRNA levels in the αGFP-AgoshR2-expressing line (Figure 3A). Next to *gfp*, 32 other genes, mainly members of

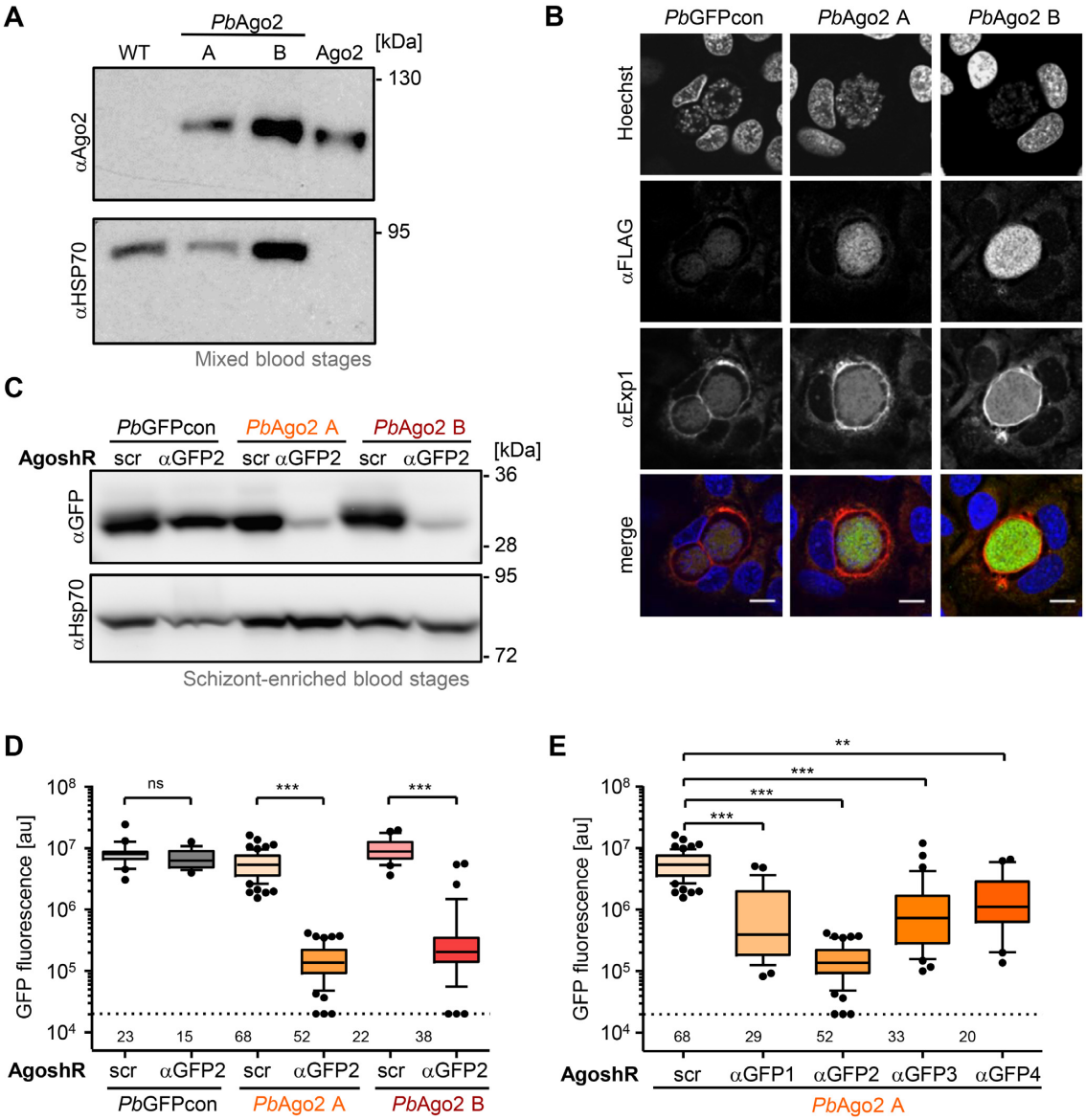

Figure 2. AgoshRNAs permit fine-tuning of *gfp* expression in an Ago2-expressing *P. berghei* line. (**A**) Western blot to detect Ago2 expression in the two *Pb*Ago2 clones. WT, wild-type *Pb*GFPcon used as negative control. Ago2, positive control (human embryonic kidney (HEK293T) cell lysate). Shown is a representative image of three replicates. (**B**) Representative immunofluorescence images (of $n = 10$) of *Pb*GFPcon and *Pb*Ago2 A and B liver stages. Human hepatoma cells (HuH7) were fixed 48 h after infection with sporozoites and stained with an anti-FLAG (recognizing the N-terminal FLAG tag of hAgo2) and an anti-EXP1 (endogenous, positive control) antibody as well as Hoechst to label nuclei. In the merge images, EXP1 is shown in red and FLAG/hAgo2 in green. Scale bars, 10 μm. (C, D) Quantification of GFP by (**C**) Western blot (representative of $n = 2$) and (**D**) microscopy (late trophozoites, $n = 3$) of *Pb*GFPcon or *Pb*Ago2 expressing αGFP-AgoshR2 (αGFP2) or scr-AgoshRNA (scr). (**E**) GFP fluorescence (late trophozoites) of *Pb*Ago2 expressing αGFP-AgoshRNAs ($n = 2$). (D, E) Whisker plots with 10–90 percentile. Dashed line, background. Numbers indicate total numbers of parasites analyzed. Statistics: (D, E) Kruskal–Wallis-test. ns, non-significant; $^{**}P < 0.01$; $^{***}P < 0.001$. au, arbitrary units; AgoshR, AgoshRNA.

the *bir*- and *fam-b*-multigene families, showed more than three-fold down-regulation upon αGFP-AgoshR2 expression (Supplementary Table S3). Notably, the vast majority of these changes were statistically non-significant ($P < 0.05$; note the substantial variation in expression between the clones) and more likely due to clonally variant gene expression rather than representing a genuine AgoshRNA-mediated effect.

Additionally, we performed a BLAST search to identify potential off-targets in the *P. berghei* transcriptome by searching for mRNA sequences with ten or more nucleotides identical to the αGFP-AgoshR2 target sequence. Based on the RNA-Seq data, we then analyzed the relative transcript expression of the 29 *P. berghei* genes with the highest sequence identity with the αGFP-AgoshR2 in our different strains (*Pb*Ago2, *Pb*Ago2 + scr-AgoshR and *Pb*Ago2 + αGFP-AgoshR2). Importantly, as shown in Figure 3B, none of these 29 genes was significantly dysregulated upon expression of the αGFP-AgoshR2, implying the absence of any detectable off-targeting even at highly similar

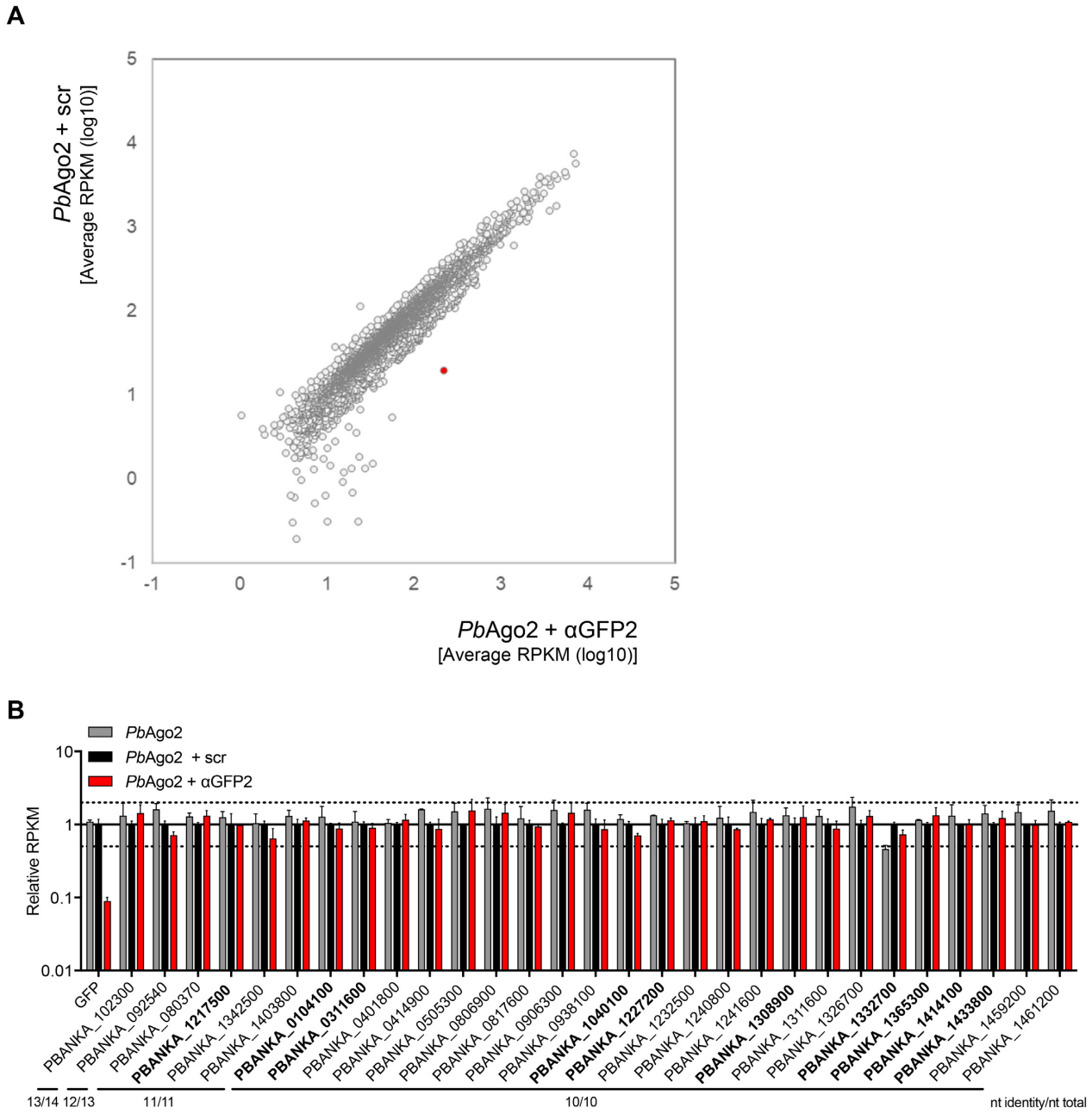

Figure 3. Minimal off-targeting observed for AgoshRNA-mediated gene silencing. (**A**) Scatter plot comparing transcript levels (reads per kilobase per million [RPKM], log10) of *Pb*Ago2 + scr-AgoshR to *Pb*Ago2 + αGFP-AgoshR2 ($n = 2$). *gfp* is highlighted in red. (**B**) Relative transcript levels of *gfp* and the top 29 *P. berghei* genes with the highest sequence identity to AgoshRNA αGFP2 (≥10 nt as identified by BLAST) in *Pb*Ago2, *Pb*Ago2 + scr and *Pb*Ago2 + αGFP2. Mean RPKM values of two biological replicates per sample were normalized to *Pb*Ago2 + scr (indicated by solid full line). The degree of sequence identity between αGFP-AgoshR2 and each gene sequence (allowing for a gap of 1 nt) is indicated below the gene IDs. Genes in bold denote targets with a 100% sequence match to the seed sequence (nt 2–8) of αGFP2. The borders of two-fold changes (up or down) are indicated by dashed lines. Data is depicted on a log scale. Error bars indicate SD.

P. berghei sequences. Further of note, these 29 targets include ten with a perfect seed match (nucleotides 2–8; highlighted in bold in Figure 3B), but even these show no signs of adverse dysregulation, substantiating the high specificity of our approach.

Hence, taken together, our consistent experimental data allow us to conclude that AgoshRNA-mediated knockdown in our engineered *Plasmodium* strain is not only efficient, but can also be specific for the targeted gene, with none to minimal off-target effects. In this context, we note that the *P. berghei* genome has a relatively low GC content (∼23.5% in coding regions). Thus, the use of GC-rich AgoshRNAs to target such an AT-rich transcriptome may underestimate the real extent of off-target effects. At the same time, it is important to point out that there are numerous 19 nt 'windows' in the *P. berghei* transcriptome that

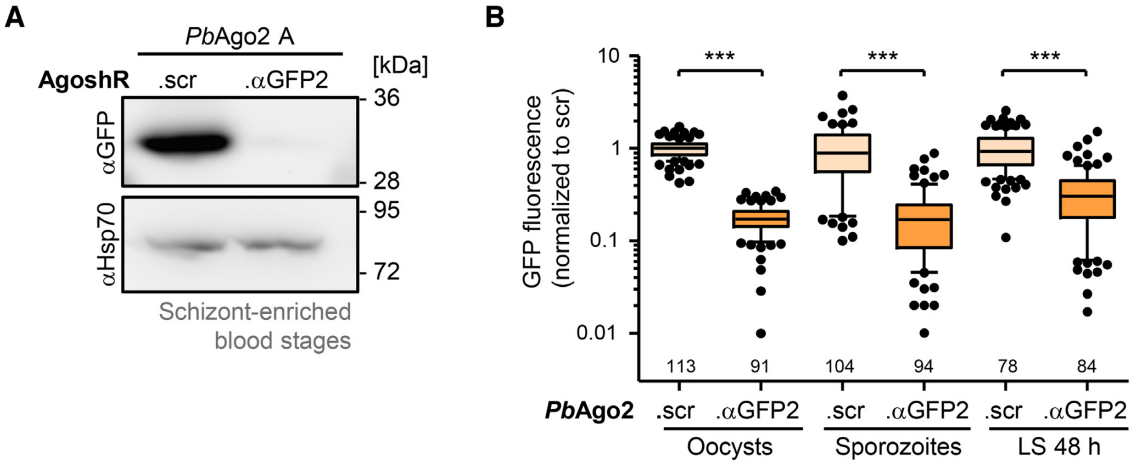

Figure 4. Constitutive expression of AgoshRNAs permits gene silencing across the malaria life cycle. (**A**) Western blot analysis of schizont-enriched samples of *Pb*Ago2.scr and *Pb*Ago2.αGFP2 (representative image from $n = 2$). (**B**) GFP fluorescence of non-erythrocytic stages of *Pb*Ago2.αGFP2 normalized to *Pb*Ago2.scr. LS, liver stages fixed at 48 h. $n = 3$, for LS $n = 2$. Whisker plots with 10–90 percentile. Dashed line, background. Numbers indicate total numbers of parasites analyzed. Statistics: (**B**) One-way ANOVA. ns, non-significant; $***P < 0.001$. au, arbitrary units.

have a high, close to 45% GC content. Therefore, in order to comprehensively address AgoshRNA off-targeting activity across all these different regions of the *Plasmodium* genome, future work should aim at conducting RNA-Seq analyses with a large array of tiled AgoshRNAs, which was beyond our present scope.

Constitutive AgoshRNA expression permits gene silencing across the malaria life cycle

Thus far, we had harnessed episomal plasmid DNAs for AgoshRNA expression. However, episomes are maintained only in the blood stages of *P. berghei* (when kept under constant drug pressure) and are lost in the mosquito stages. To study the feasibility to also target genes in the mosquito and liver stages of *Pb*Ago2, we stably integrated expression cassettes for scr-AgoshR or αGFP-AgoshR2 under the ubiquitously active U6 promoter (Supplementary Figure S6A-B). Constitutive AgoshRNA expression did not impair the blood-stage growth rate of the engineered parasites (Supplementary Figure S6C). As hoped for, we measured a strong GFP knockdown in *Pb*Ago2.αGFP2 blood stages as compared to the *Pb*Ago2.scr control (Figure 4A). Moreover, following *Pb*Ago2.αGFP2 transmission to mosquitoes, we observed a marked GFP reduction in oocysts and salivary gland sporozoites imaged at day 13 or 18 after transmission, respectively, as well as in liver stages (Figure 4B, Supplementary Figure S7). Together, these data imply that mRNA knockdown via integrated AgoshRNAs is indeed possible during all parasite life cycle stages.

AgoshRNA-mediated silencing of an endogenous gene phenocopies a full knockout

We then aimed to inhibit an endogenous *P. berghei* target and chose the *Plasmodium* perforin-like protein 2 (PPLP2) for this purpose. Its knockout causes a defect during exflagellation (37,38), i.e. the process by which the male gametocyte divides into eight flagellated gametes that emerge from the host red blood cell to fertilize female gametes. As PPLP2 is required for membrane lysis during this process, PPLP2-deficient parasites are trapped within the erythrocyte membrane. Thus, instead of eight individual flagella, one large superflagellum is detected microscopically. We expressed three different AgoshRNAs against PPLP2 in *Pb*Ago2 and measured PPLP2 mRNA levels via quantitative real-time PCR, as antibodies for PPLP2 protein detection via Western blotting were not available. Two of the AgoshRNAs, αPPLP2-AgoshRNA 1 and 2, reduced PPLP2 mRNA levels significantly to 38% or 25% of control parasites expressing scr-AgoshR, respectively (Figure 5A). Moreover, parasites expressing these αPPLP2 AgoshRNAs formed a superflagellum (Figure 5B and C). Together, this corroborates the capacity of our novel approach to suppress endogenous genes in *Plasmodium*, and exemplifies how AgoshRNA-mediated knockdown can even phenocopy a full knockout.

Interestingly, the extent of PPLP2 knockdown correlated with a striking reduction of the overall exflagellation rate (Figure 5D), which recapitulates the phenotype of a PPLP2-deficient *P. falciparum* line (38). In contrast, exflagellation rates remained constant after PPLP2 knockout in *P.* berghei (37). A possible explanation is that in *P. berghei*, gametocyte egress and formation of superflagella are also observed after knockout of other genes, such as *Pb*GEST (39), implying a complex biology underlying *P. berghei* exflagellation. Consequently, it is tempting to speculate that the previous full PPLP2 knockout in *P. berghei* may have triggered a compensatory genetic network that partially buffered against the associated deleterious phenotypes. This genetic compensation might be delayed and/or diminished following a milder gene knockdown, which can, in turn, facilitate the manifestation of a stronger phenotype. In fact, we note extensive data exemplifying this paradoxon, *i.e.*, more severe phenotypes after target gene knockdown as compared to knockout, in numerous other eukaryotic species (e.g. (40)). While more work is required to dissect the mechanisms in the case of PPLP2, our data may therefore already indicate another benefit of our new strategy over existing genetic

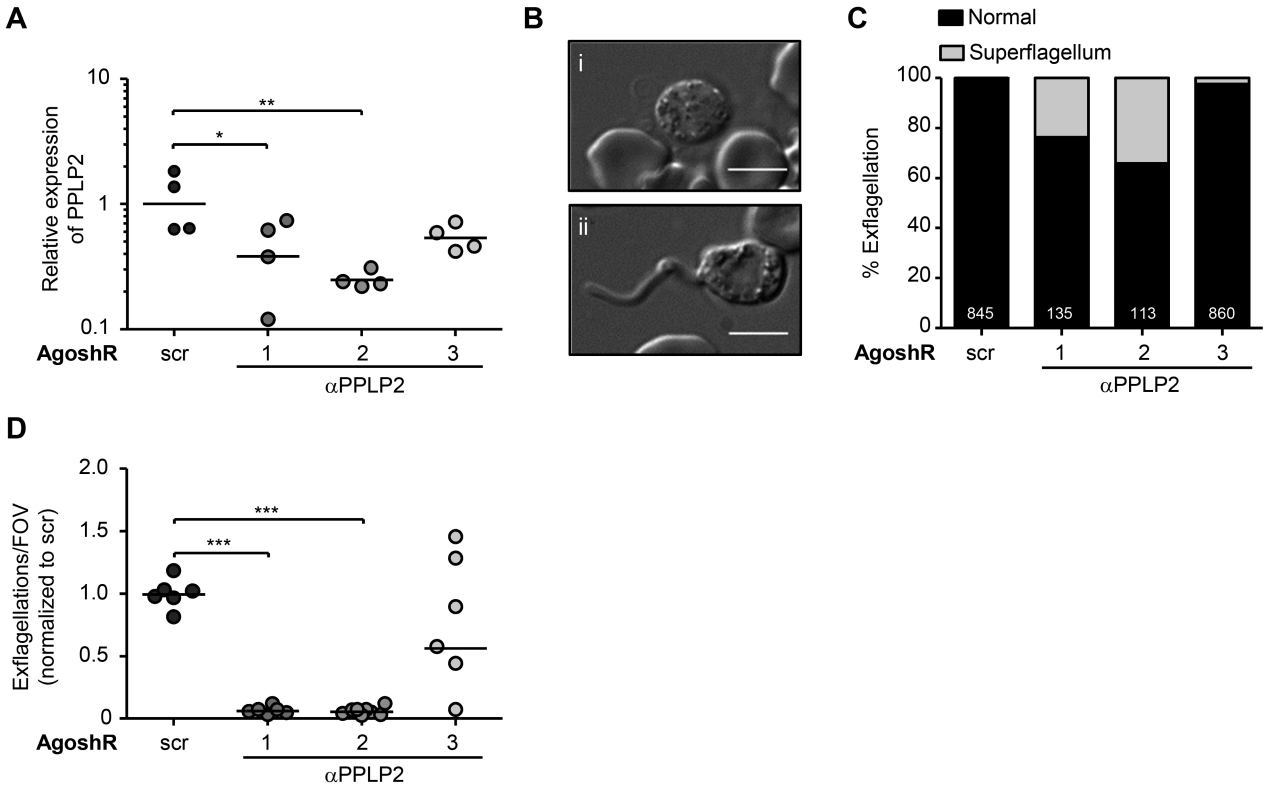

Figure 5. AgoshRNA-mediated silencing of an endogenous gene phenocopies a full knockout. (**A**) Quantification of PPLP2 mRNA in *Pb*Ago2 expressing αPPLP2-AgoshRNAs normalized to scr-AgoshRNA ($n = 2$, two mice each). (**B**) Representative images of (i) a normal exflagellating gametocyte and (ii) an abnormal exflagellating gametocyte forming a superflagellum. Scale bar, 10 μm. (**C**) Proportion of normal (eight flagella) and abnormal (superflagellum) exflagellation events observed for *Pb*Ago2 expressing scr-AgoshR or αPPLP2-AgoshRNAs. Numbers in the bars indicate total numbers of events observed. (**D**) Quantification of exflagellation events per field of view (FOV) ($n = 3$, two mice each). Statistics: (A, D) One-way-ANOVA. $^{*}P < 0.05$; $^{**}P < 0.01$; $^{***}P < 0.001$.

technologies in *Plasmodium* that require the generation of stable knockout mutants.

Independent and robust AgoshRNA-mediated silencing of a second endogenous gene

Our notion of the possibility to achieve differential knockdowns to varying levels suggested that our strategy might permit targeting of a blood-stage essential gene, whose partial knockdown may be compatible with parasite survival. To test this hypothesis, we chose the exported protein 1 (EXP1) as a target, i.e. a dominant antigen in many immune responses and a major vaccine candidate. This protein is located to the parasitophorous vacuole membrane of blood-stage as well as liver-stage parasites and is a key factor for *Plasmodium* asexual development (41–43). Moreover, while EXP1 is refractory to gene deletion, our own previous studies with truncated versions have implied an interaction of its C-terminus with the host cell factor ApoH1 (21). Other than this, the exact function of EXP1 is not clearly defined but is probably very complex and the subject of ongoing work in our laboratory and others (44,45).

We first designed three different AgoshRNAs (Supplementary Table S2) against EXP1 and episomally transfected them into *Pb*Ago2. Mice became blood-stage-positive one to two weeks after transfection. Following confirmation that all parasites retained the episome (as evidenced by mCherry fluorescence), we analyzed EXP1 expression by Western blotting (Figure 6A). Notably, signal quantification revealed a robust reduction of EXP1 expression to ∼40–50% for the AgoshRNAs αEXP1–1 and 2 as compared to the scrambled AgoshRNA control, whereas AgoshRNA αEXP1–3 was inert (Figure 6A-B). We then stably transfected one of the two potent AgoshRNAs (αEXP1–1) into *Pb*Ago2 and generated two independent clones. In both of these stable AgoshRNA transfectants, we again found substantial EXP1 inhibition of over 50% on the protein level (Figure 6C and D).

This high efficiency is remarkable, considering that—as noted—EXP1 is an essential factor for *Plasmodium* asexual development and that its gene cannot be deleted. Hence, these results not only further illustrate the potential of our technology to inhibit endogenous *Plasmodium* genes, but concurrently also exemplify a case where a partial knockdown strategy such as the one reported here is particularly beneficial, as a full knockout of EXP1 would have been lethal.

Stage-specific expression of Ago2 enables temporally controlled gene silencing

Finally, we investigated the possibility to restrict Ago2 expression and thus gene knockdown to specific stages in the parasite life cycle. Therefore, we generated a *P. berghei* line

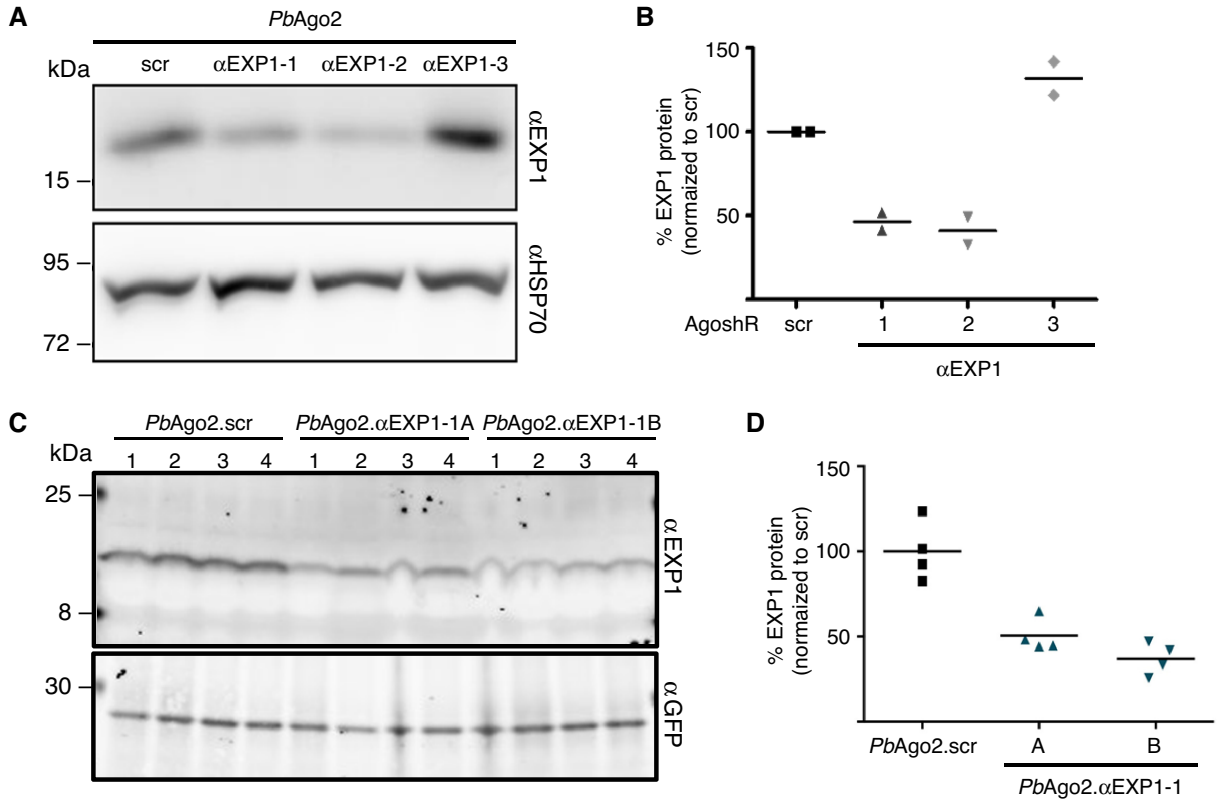

Figure 6. Knockdown of EXP1 in *Pb*Ago2 parasites expressing αEXP1-AgoshRNAs (A, B) episomally or (C, D) from an integrated locus. (**A**) Schizont-enriched samples of *Pb*Ago2 episomally expressing AgoshRscr or αEXP1-AgoshR1 to 3 (αEXP1–1 to -3) were analyzed by Western blotting probing for either EXP1 or HSP70 (loading control). Shown is one representative blot of two technical replicates. (**B**) Quantification of Western blot signals from panel A (plus replicate). Band intensities were determined with ImageJ, and the EXP1 signals were normalized to the HSP70 signal. The *Pb*Ago2 + scr sample served as control for normalization and was set to 100%. Each dot represents the signal of an individual technical replicate. (**C**) Schizont-enriched samples of *Pb*Ago2.αEXP1–1 parasites were analyzed by Western blotting probing for either EXP1 or GFP (loading control). Shown are four technical replicates (1–4) of two independent clones A and B of *Pb*Ago2.αEXP1–1 and one clone of *Pb*Ago2.scr. (**D**) Quantification of Western blot signals from panel C. See panel B for details.

expressing Ago2 from the liver stage-specific promoter of the *LISP2* gene (Supplementary Figure S8A). Indeed, the resulting line Pb_{LISP2}Ago2 expresses Ago2 in liver stages but no longer in blood stages (Figure 7A and B). Notably, Pb_{LISP2}Ago2 exhibits no growth defects at any stage of the life cycle (Supplementary Figure S8B–F), implying that restricting Ago2 expression to the liver stage has helped to circumvent the impairment noted in *Pb*Ago2 (outside the liver stage, Supplementary Figure S2). Integration of αGFP-AgoshR2 (Supplementary Figure S8G-H) did not result in reduced GFP levels in blood stages, oocysts or sporozoites (Figure 7C and D, Supplementary Figure S9A and B), indicating that the *LISP2* promoter is completely inactive in those stages. In contrast, we observed a significant GFP knockdown in liver stages, which peaked at 48 h post-invasion (65% reduction, Figure 7D, Supplementary Figure S9C), coinciding with the reported activity of the *LISP2* promoter (46). This exemplifies how transcriptionally restricting the non-canonical RNAi pathway to a defined parasite stage can enable temporally controlled gene knockdown in *Plasmodium*.

The possibility to direct gene knockdown to a selected stage of the life cycle by controlling Ago2 expression is particularly beneficial for the dissection of blood stage-essential genes. To our knowledge, the only other presently available genetic strategies that allow for target modulation at a given life cycle stage are either promoter exchange (e.g. (47)) or the Flp/FRT system, where stage-specific expression of the Flp recombinase leads to excision of the FRT-flanked gene of interest (48). However, both of these systems do not allow for fine-tuning of gene expression. In the future, it could be rewarding to further enhance our new parasite lines by juxtaposing ubiquitous or stage-specific Ago2 promoters with conditional systems, e.g. a tetracycline repressor (49), to render target knockdown inducible and to thus additionally facilitate the study of essential genes.

CONCLUSION

Here, we have introduced RNAi technology into the *Plasmodium* field and have created transgenic parasite lines that should accelerate basic and applied malaria research alike. Noteworthy from a technical perspective is our high rate of success with AgoshRNA design, with nine out of ten candidates being functional and eight significantly inhibiting their cognate target mRNA. In addition, we have tested

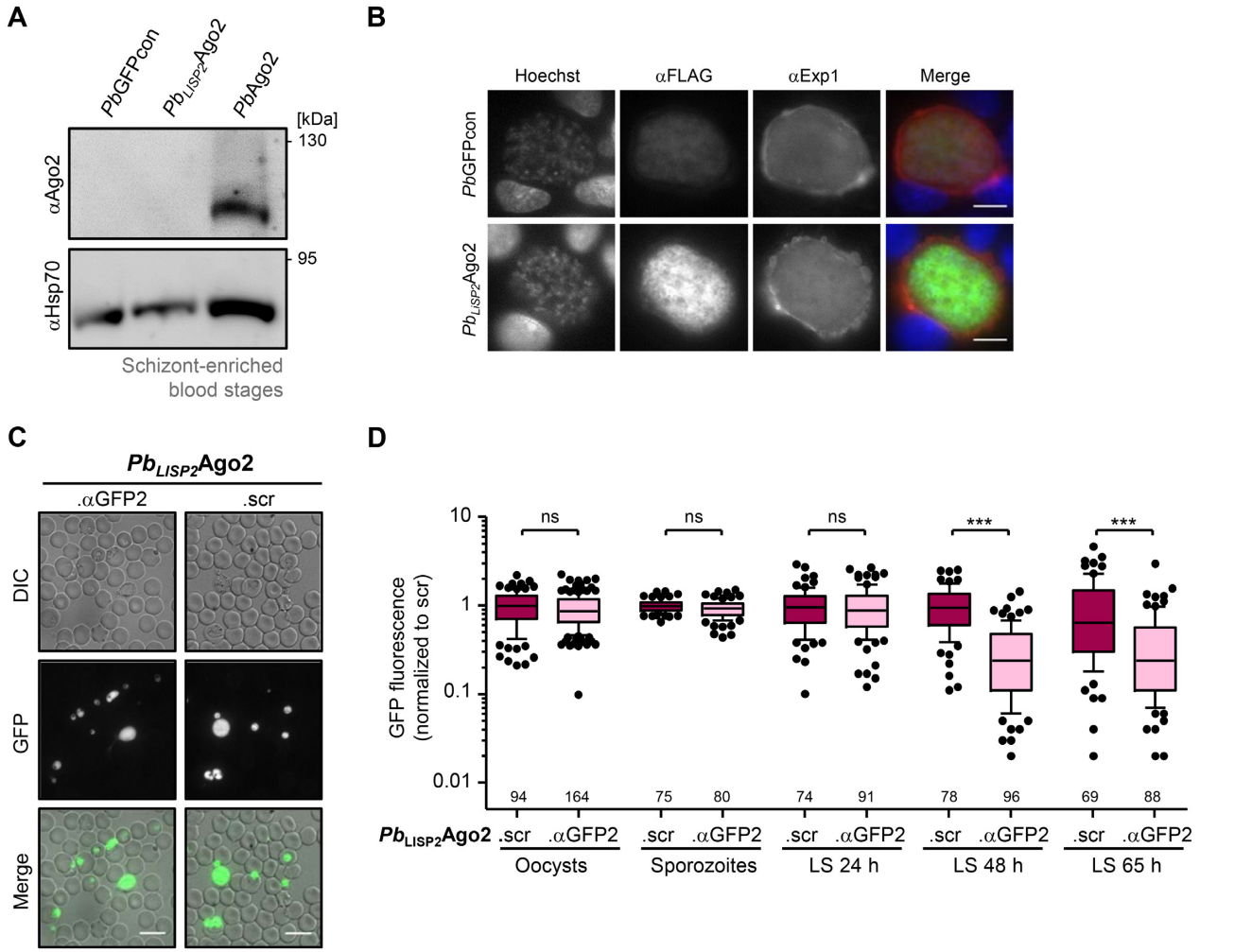

Figure 7. Stage-specific expression of Ago2 restricts gene silencing to the liver stage. (**A**) Western blot of schizont-enriched samples probed for Ago2 and Hsp70 as loading control (representative image of $n = 2$). (**B**) Representative immunofluorescence images of *Pb*GFPcon and Pb_{LISP2}Ago2. HuH7 cells were fixed 48 h after infection with sporozoites and stained with an anti-FLAG (green) and an anti-EXP1 (red) antibody as well as Hoechst to label nuclei. Scale bars, 10 μm. (**C**) Microscopy of Pb_{LISP2}Ago2 blood stages. Scale bar, 10 μm. (**D**) GFP fluorescence of non-erythrocytic stages of Pb_{LISP2}Ago2.αGFP2 normalized to Pb_{LISP2}Ago2.scr ($n = 2$). Numbers indicate total numbers of parasites analyzed. LS, liver stages (fixed and stained at indicated time points post-infection). Whisker plot with 10–90 percentile. Statistics: (**D**) one-way-ANOVA. ns, non-significant; $***P < 0.001$.

seven other AgoshRNAs in previous work in mammalian cells (50) and found all to be functional as well, representing an overall success rate of 94% (16 out of 17). As a whole, and combined with our reassuring data on AgoshRNA specificity, these results illustrate that the technology introduced here is ready-to-use and is very likely easily adapted in other laboratories contemplating knockdown experiments in *P. berghei*. Furthermore, we note our (Berkhout laboratory) recent set of independent publications on comprehensive rules for the design of second-generation AgoshRNAs with improved biogenesis and efficiency (51–54). As a whole, this is very encouraging as it suggests the feasibility to perform multiplexed RNAi screens in *Plasmodium*, akin to those reported in inherently RNAi-competent parasites such as *Trypanosoma brucei* (55).

We foresee that our novel strategy will be welcome as a valuable addition to the currently available tools to study *Plasmodium* gene function. A particularly attractive feature that complements existing technology is its ability to achieve intermediate gene knockdowns. We acknowledge that for some genes, a partial knockdown might not suffice to observe a clear phenotype; rather, these genes might require a full knockout. Nonetheless, for other genes, intermediate knockdown strategies are highly beneficial as they enable the investigation of dose-dependent effects of gene suppression. This is exemplified here by our knockdown of PPLP2, where the extent of the knockdown on the RNA level correlated well with the proportion of parasites developing a superflagellum. Similar titratable gene knockdown strategies exist for *P. falciparum,* e.g. the *glms* ribozyme system (1). However, they have found only limited application in rodent models and require the addition of drugs, which is particularly difficult in non-erythrocytic stages of the life cycle. Also notable in this context is an elegant recent study describing the use of CRISPRi to modulate gene expression in *P. yoelli,* by using a g(uide)RNA-targeted, catalyti-

cally inactive Cas9 protein to inhibit gene expression and to thereby achieve different knockdown levels depending on the position of the gRNA (56). In contrast to the system presented here, though, this strategy is currently not applicable to mosquito and liver stages of the parasite due to the transient Cas9 expression from an episomal plasmid.

As with other strategies that involve genetic manipulation of the parasite to control gene expression, compensatory mutations may arise during the time needed to generate the parasite line and may potentially confound the observed phenotype. To avoid such compensatory effects, future improvements of the systems should include an inducible element for either Ago2 or AgoshRNA expression, such as the Tet-Repressor system (57). This would also enable the study of essential genes, whose knockdown might be detrimental to asexual parasite growth and, thus, prevent the recovery of transfectants constitutively expressing active AgoshRNAs. Importantly, such inducible elements are not necessary when using the stage-specific Pb_{LISP2}Ago2 line, as gene expression in blood stages will remain unperturbed.

Altogether, we thus envision significant potential of this strategy and the transgenic *Plasmodium* lines reported here, ranging from fundamental gene annotation in a low- or high-throughput manner, to discovery of new antimalarial drug and vaccine candidates. Furthermore, our paradigm that RNAi-negative organisms can be rendered RNAi-competent by sole introduction of Ago2 and AgoshRNA may also find broad applicability in other species such as *Saccharomyces cerevisiae*.

DATA AVAILABILITY

Raw RNA-Seq data have been deposited in NCBI's Gene Expression Omnibus and are accessible through GEO Series accession number GSE95534.

SUPPLEMENTARY DATA

Supplementary Data are available at NAR Online.

ACKNOWLEDGEMENTS

The authors thank Christian Sommerauer for mosquito breeding, Freddy Frischknecht for providing access to a widefield fluorescence microscope, and Mirko Singer (all Heidelberg University Hospital, Center for Infectious Diseases, Integrative Parasitology, Heidelberg, Germany) for providing the ImageJ macro to quantify fluorescence signals. In addition, F.H., A.-K.M. and D.G. thank members of the Mueller and Grimm laboratories for critical reading of the manuscript.

Author contributions: A.-K.M. and D.G. initiated and supervised the study; F.H., A.-K.M. and D.G. designed the experiments; F.H. performed most experiments; V.M. generated and characterized the Pb_{LISP2}Ago2 line; S.A.-K.F. and R.B. performed RNA-Seq and analyzed resulting data; D.K. generated the first *Pb*Ago2 line; E.H.C. and B.B. assisted with the design of the αGFP-AgoshRNAs; F.H., A.-K.M. and D.G. wrote and revised the manuscript with contributions by all authors.

FUNDING

German Research Foundation (DFG) [EXC81 (Cluster of Excellence CellNetworks) to F.H. and D.G., Collaborative Research Center SFB1129 (TP 2 to F.H., A.-K.M. and D.G., Projektnummer 240245660), Collaborative Research Center TRR179 (TP 18 to D.G., Projektnummer 272983813), SPP 1580 to A.-K.M.]; Innovation fund Frontier from Heidelberg University [to F.H., A.-K.M. and D.G.]; German Center for Infection Research (DZIF) [maternity leave stipend to A.-K.M.]; Netherlands Organization for Scientific Research [NWO-Vidi 864.11.007 to R.B.]. F.H. appreciates support and mentoring by the Heidelberg Biosciences International Graduate School (HBIGS) at Heidelberg University. Funding for open access charge: Heidelberg University Hospital.

Conflict of interest statement. None declared.

REFERENCES

1. de Koning-Ward,T.F., Gilson,P.R. and Crabb,B.S. (2015) Advances in molecular genetic systems in malaria. *Nat. Rev. Microbiol.*, **13**, 373–387.
2. Bushell,E., Gomes,A.R., Sanderson,T., Anar,B., Girling,G., Herd,C., Metcalf,T., Modrzynska,K., Schwach,F., Martin,R.E. *et al.* (2017) Functional profiling of a plasmodium genome reveals an abundance of essential genes. *Cell*, **170**, 260–272.
3. Zhang,M., Wang,C., Otto,T.D., Oberstaller,J., Liao,X., Adapa,S.R., Udenze,K., Bronner,I.F., Casandra,D., Mayho,M. *et al.* (2018) Uncovering the essential genes of the human malaria parasite Plasmodium falciparum by saturation mutagenesis. *Science*, **360**, eaap7847.
4. Grimm,D. (2009) Small silencing RNAs: state-of-the-art. *Adv. Drug Deliv. Rev.*, **61**, 672–703.
5. Baum,J., Papenfuss,A.T., Mair,G.R., Janse,C.J., Vlachou,D., Waters,A.P., Cowman,A.F., Crabb,B.S. and de Koning-Ward,T.F. (2009) Molecular genetics and comparative genomics reveal RNAi is not functional in malaria parasites. *Nucleic Acids Res.*, **37**, 3788–3798.
6. Herrera-Carrillo,E. and Berkhout,B. (2017) Dicer-independent processing of small RNA duplexes: mechanistic insights and applications. *Nucleic Acids Res.*, **45**, 10369–10379.
7. Liu,Y.P., Schopman,N.C. and Berkhout,B. (2013) Dicer-independent processing of short hairpin RNAs. *Nucleic Acids Res.*, **41**, 3723–3733.
8. Herrera-Carrillo,E., Harwig,A., Liu,Y.P. and Berkhout,B. (2014) Probing the shRNA characteristics that hinder Dicer recognition and consequently allow Ago-mediated processing and AgoshRNA activity. *RNA*, **20**, 1410–1418.
9. Grimm,D., Streetz,K.L., Jopling,C.L., Storm,T.A., Pandey,K., Davis,C.R., Marion,P., Salazar,F. and Kay,M.A. (2006) Fatality in mice due to oversaturation of cellular microRNA/short hairpin RNA pathways. *Nature*, **441**, 537–541.
10. Kooij,T.W., Rauch,M.M. and Matuschewski,K. (2012) Expansion of experimental genetics approaches for Plasmodium berghei with versatile transfection vectors. *Mol. Biochem. Parasitol.*, **185**, 19–26.
11. Schurmann,N., Trabuco,L.G., Bender,C., Russell,R.B. and Grimm,D. (2013) Molecular dissection of human Argonaute proteins by DNA shuffling. *Nat. Struct. Mol. Biol.*, **20**, 818–826.
12. Helm,S., Lehmann,C., Nagel,A., Stanway,R.R., Horstmann,S., Llinas,M. and Heussler,V.T. (2010) Identification and characterization of a liver stage-specific promoter region of the malaria parasite Plasmodium. *PLoS One*, **5**, e13653.
13. Liu,Y.P., Karg,M., Herrera-Carrillo,E. and Berkhout,B. (2015) Towards antiviral shrnas based on the agoshrna design. *PLoS One*, **10**, e0128618.
14. Grimm,D. (2002) Production methods for gene transfer vectors based on adeno-associated virus serotypes. *Methods*, **28**, 146–157.
15. Grimm,D., Lee,J.S., Wang,L., Desai,T., Akache,B., Storm,T.A. and Kay,M.A. (2008) In vitro and in vivo gene therapy vector evolution via multispecies interbreeding and retargeting of adeno-associated viruses. *J. Virol.*, **82**, 5887–5911.

16. Janse,C.J., Ramesar,J. and Waters,A.P. (2006) High-efficiency transfection and drug selection of genetically transformed blood stages of the rodent malaria parasite Plasmodium berghei. *Nat. Protoc.*, **1**, 346–356.
17. Orr,R.Y., Philip,N. and Waters,A.P. (2012) Improved negative selection protocol for Plasmodium berghei in the rodent malarial model. *Malar. J.*, **11**, 103.
18. Sriprawat,K., Kaewpongsri,S., Suwanarusk,R., Leimanis,M.L., Lek-Uthai,U., Phyo,A.P., Snounou,G., Russell,B., Renia,L. and Nosten,F. (2009) Effective and cheap removal of leukocytes and platelets from Plasmodium vivax infected blood. *Malar. J.*, **8**, 115.
19. Tsuji,M., Mattei,D., Nussenzweig,R.S., Eichinger,D. and Zavala,F. (1994) Demonstration of heat-shock protein 70 in the sporozoite stage of malaria parasites. *Parasitol. Res.*, **80**, 16–21.
20. Rudel,S., Flatley,A., Weinmann,L., Kremmer,E. and Meister,G. (2008) A multifunctional human Argonaute2-specific monoclonal antibody. *RNA*, **14**, 1244–1253.
21. Sa,E.C.C., Nyboer,B., Heiss,K., Sanches-Vaz,M., Fontinha,D., Wiedtke,E., Grimm,D., Przyborski,J.M., Mota,M.M., Prudencio,M. *et al.* (2017) Plasmodium berghei exp-1 interacts with host apolipoprotein h during plasmodium liver-stage development. *Proc. Natl. Acad. Sci. U.S.A.*, **114**, E1138–E1147.
22. Beetsma,A.L., van de Wiel,T.J., Sauerwein,R.W. and Eling,W.M. (1998) Plasmodium berghei ANKA: purification of large numbers of infectious gametocytes. *Exp. Parasitol.*, **88**, 69–72.
23. Drew,D.R. and Reece,S.E. (2007) Development of reverse-transcription PCR techniques to analyse the density and sex ratio of gametocytes in genetically diverse Plasmodium chabaudi infections. *Mol. Biochem. Parasitol.*, **156**, 199–209.
24. Pfaffl,M.W. (2001) A new mathematical model for relative quantification in real-time RT-PCR. *Nucleic Acids Res.*, **29**, e45.
25. Hoeijmakers,W.A., Bartfai,R. and Stunnenberg,H.G. (2013) Transcriptome analysis using RNA-Seq. *Methods Mol. Biol.*, **923**, 221–239.
26. Kensche,P.R., Hoeijmakers,W.A., Toenhake,C.G., Bras,M., Chappell,L., Berriman,M. and Bartfai,R. (2016) The nucleosome landscape of Plasmodium falciparum reveals chromatin architecture and dynamics of regulatory sequences. *Nucleic Acids Res.*, **44**, 2110–2124.
27. Franke-Fayard,B., Trueman,H., Ramesar,J., Mendoza,J., van der Keur,M., van der Linden,R., Sinden,R.E., Waters,A.P. and Janse,C.J. (2004) A Plasmodium berghei reference line that constitutively expresses GFP at a high level throughout the complete life cycle. *Mol. Biochem. Parasitol.*, **137**, 23–33.
28. Li,H. and Durbin,R. (2009) Fast and accurate short read alignment with Burrows-Wheeler transform. *Bioinformatics*, **25**, 1754–1760.
29. Herrera-Carrillo,E., Harwig,A. and Berkhout,B. (2015) Toward optimization of AgoshRNA molecules that use a non-canonical RNAi pathway: variations in the top and bottom base pairs. *RNA Biol.*, **12**, 447–456.
30. Hliscs,M., Nahar,C., Frischknecht,F. and Matuschewski,K. (2013) Expression profiling of Plasmodium berghei HSP70 genes for generation of bright red fluorescent parasites. *PLoS One*, **8**, e72771.
31. Chakrabarti,K., Pearson,M., Grate,L., Sterne-Weiler,T., Deans,J., Donohue,J.P. and Ares,M. Jr (2007) Structural RNAs of known and unknown function identified in malaria parasites by comparative genomics and RNA analysis. *RNA*, **13**, 1923–1939.
32. Jackson,A.L., Bartz,S.R., Schelter,J., Kobayashi,S.V., Burchard,J., Mao,M., Li,B., Cavet,G. and Linsley,P.S. (2003) Expression profiling reveals off-target gene regulation by RNAi. *Nat. Biotechnol.*, **21**, 635–637.
33. Mockenhaupt,S., Grosse,S., Rupp,D., Bartenschlager,R. and Grimm,D. (2015) Alleviation of off-target effects from vector-encoded shRNAs via codelivered RNA decoys. *Proc. Natl. Acad. Sci. U.S.A.*, **112**, E4007–E4016.
34. Herrera-Carrillo,E., Harwig,A. and Berkhout,B. (2017) Silencing of HIV-1 by AgoshRNA molecules. *Gene Ther.*, **24**, 453–461.
35. Mair,G.R., Lasonder,E., Garver,L.S., Franke-Fayard,B.M., Carret,C.K., Wiegant,J.C., Dirks,R.W., Dimopoulos,G., Janse,C.J. and Waters,A.P. (2010) Universal features of post-transcriptional gene regulation are critical for Plasmodium zygote development. *PLoS Pathog.*, **6**, e1000767.
36. Chu,C.Y. and Rana,T.M. (2006) Translation repression in human cells by microRNA-induced gene silencing requires RCK/p54. *PLoS Biol.*, **4**, e210.
37. Deligianni,E., Morgan,R.N., Bertuccini,L., Wirth,C.C., Silmon de Monerri,N.C., Spanos,L., Blackman,M.J., Louis,C., Pradel,G. and Siden-Kiamos,I. (2013) A perforin-like protein mediates disruption of the erythrocyte membrane during egress of Plasmodium berghei male gametocytes. *Cell Microbiol.*, **15**, 1438–1455.
38. Wirth,C.C., Glushakova,S., Scheuermayer,M., Repnik,U., Garg,S., Schaack,D., Kachman,M.M., Weissbach,T., Zimmerberg,J., Dandekar,T. *et al.* (2014) Perforin-like protein PPLP2 permeabilizes the red blood cell membrane during egress of Plasmodium falciparum gametocytes. *Cell Microbiol.*, **16**, 709–733.
39. Talman,A.M., Lacroix,C., Marques,S.R., Blagborough,A.M., Carzaniga,R., Menard,R. and Sinden,R.E. (2011) PbGEST mediates malaria transmission to both mosquito and vertebrate host. *Mol. Microbiol.*, **82**, 462–474.
40. Rossi,A., Kontarakis,Z., Gerri,C., Nolte,H., Holper,S., Kruger,M. and Stainier,D.Y. (2015) Genetic compensation induced by deleterious mutations but not gene knockdowns. *Nature*, **524**, 230–233.
41. Hall,R., McBride,J., Morgan,G., Tait,A., Zolg,J.W., Walliker,D. and Scaife,J. (1983) Antigens of the erythrocytes stages of the human malaria parasite Plasmodium falciparum detected by monoclonal antibodies. *Mol. Biochem. Parasitol.*, **7**, 247–265.
42. Simmons,D., Woollett,G., Bergin-Cartwright,M., Kay,D. and Scaife,J. (1987) A malaria protein exported into a new compartment within the host erythrocyte. *EMBO J.*, **6**, 485–491.
43. Sanchez,G.I., Rogers,W.O., Mellouk,S. and Hoffman,S.L. (1994) Plasmodium falciparum: exported protein-1, a blood stage antigen, is expressed in liver stage parasites. *Exp. Parasitol.*, **79**, 59–62.
44. Lisewski,A.M., Quiros,J.P., Ng,C.L., Adikesavan,A.K., Miura,K., Putluri,N., Eastman,R.T., Scanfeld,D., Regenbogen,S.J., Altenhofen,L. *et al.* (2014) Supergenomic network compression and the discovery of EXP1 as a glutathione transferase inhibited by artesunate. *Cell*, **158**, 916–928.
45. Wolanin,K., Fontinha,D., Sanches-Vaz,M., Nyboer,B., Heiss,K., Mueller,A.K. and Prudencio,M. (2019) A crucial role for the C-terminal domain of exported protein 1 during the mosquito and hepatic stages of the Plasmodium berghei life cycle. *Cell Microbiol.*, **21**, e13088.
46. De Niz,M., Helm,S., Horstmann,S., Annoura,T., Del Portillo,H.A., Khan,S.M. and Heussler,V.T. (2015) In vivo and in vitro characterization of a Plasmodium liver stage-specific promoter. *PLoS One*, **10**, e0123473.
47. Laurentino,E.C., Taylor,S., Mair,G.R., Lasonder,E., Bartfai,R., Stunnenberg,H.G., Kroeze,H., Ramesar,J., Franke-Fayard,B., Khan,S.M. *et al.* (2011) Experimentally controlled downregulation of the histone chaperone FACT in Plasmodium berghei reveals that it is critical to male gamete fertility. *Cell Microbiol.*, **13**, 1956–1974.
48. Combe,A., Giovannini,D., Carvalho,T.G., Spath,S., Boisson,B., Loussert,C., Thiberge,S., Lacroix,C., Gueirard,P. and Menard,R. (2009) Clonal conditional mutagenesis in malaria parasites. *Cell Host Microbe.*, **5**, 386–396.
49. Pino,P., Sebastian,S., Kim,E.A., Bush,E., Brochet,M., Volkmann,K., Kozlowski,E., Llinas,M., Billker,O. and Soldati-Favre,D. (2012) A tetracycline-repressible transactivator system to study essential genes in malaria parasites. *Cell Host Microbe.*, **12**, 824–834.
50. Borner,K., Niopek,D., Cotugno,G., Kaldenbach,M., Pankert,T., Willemsen,J., Zhang,X., Schurmann,N., Mockenhaupt,S., Serva,A. *et al.* (2013) Robust RNAi enhancement via human Argonaute-2 overexpression from plasmids, viral vectors and cell lines. *Nucleic Acids Res.*, **41**, e199.
51. Gao,Z., Berkhout,B. and Herrera-Carrillo,E. (2019) Boosting AgoshRNA activity by optimized 5′-terminal nucleotide selection. *RNA Biol.*, **16**, 890–898.
52. Herrera-Carrillo,E., Gao,Z. and Berkhout,B. (2019) Influence of a 3′ Terminal Ribozyme on AgoshRNA Biogenesis and Activity. *Mol. Ther. Nucleic Acids*, **16**, 452–462.
53. Herrera-Carrillo,E., Gao,Z.L., Harwig,A., Heemskerk,M.T. and Berkhout,B. (2017) The influence of the 5-terminal nucleotide on AgoshRNA activity and biogenesis: importance of the polymerase III transcription initiation site. *Nucleic Acids Res.*, **45**, 4036–4050.

54. Herrera-Carrillo,E., Harwig,A. and Berkhout,B. (2017) Influence of the loop size and nucleotide composition on AgoshRNA biogenesis and activity. *RNA Biol.*, **14**, 1559–1569.
55. Alsford,S., Turner,D.J., Obado,S.O., Sanchez-Flores,A., Glover,L., Berriman,M., Hertz-Fowler,C. and Horn,D. (2011) High-throughput phenotyping using parallel sequencing of RNA interference targets in the African trypanosome. *Genome Res.*, **21**, 915–924.
56. Walker,M.P. and Lindner,S.E. (2019) Ribozyme-mediated, multiplex CRISPR gene editing and CRISPR interference (CRISPRi) in rodent-infectious Plasmodium yoelii. *J. Biol. Chem.*, **294**, 9555–9566.
57. Meissner,M., Krejany,E., Gilson,P.R., de Koning-Ward,T.F., Soldati,D. and Crabb,B.S. (2005) Tetracycline analogue-regulated transgene expression in Plasmodium falciparum blood stages using Toxoplasma gondii transactivators. *Proc. Natl. Acad. Sci. U.S.A.*, **102**, 2980–2985.